

# Reaction Mechanism of Arsenic and Nitrogen Oxides in Coal Combustion

Haoying Duan

Liaoning Jiamao Energy Chemical Co., Ltd., duanhy@piscomed.com

**Abstract:** The reaction mechanism of arsenic and nitrogen oxides (N<sub>2</sub>O, NO<sub>2</sub> and NO) was studied by using density functional theory of quantum chemistry B3LYP method. All parameters optimize the geometric configuration of each reactant, intermediate, transition state and product. The authenticity of intermediate and transition state is confirmed by frequency analysis, and the transition state is further determined by calculation of intrinsic reaction coordinate (IRC). In order to obtain more accurate energy information, the single-point energy of each structure is calculated at B2PLYP level, and its reaction mechanism is deeply analyzed through kinetic parameters. The results show that the reaction energy barrier between arsenic and three nitrogen oxides (N<sub>2</sub>O, NO<sub>2</sub> and NO) is 78.45, 2.58, 155.85kJ/mol respectively. At 298-1800 K, each reaction rate increases with the increase of temperature. Due to the low reaction energy barrier between arsenic and NO<sub>2</sub>, the reaction rate is greater than 1012 cm<sup>3</sup>/(mol s), indicating that the reaction is easy to occur and extremely fast. Arsenic reacts with N<sub>2</sub>O and NO at 298-900 K, and the reaction rate increases obviously with the increase of temperature. When the temperature rises further, its increasing trend slows down.

**Keywords:** Coal combustion; Arsenic; Nitrogen oxides; Density functional theory; Dynamics

Coal is the main energy source in China, and the environmental pollution caused by coal combustion is highly valued [1]. In the process of pulverized coal combustion, not only a large number of conventional pollutants (SO<sub>x</sub>, NO<sub>x</sub>, particulate matter, etc.) are generated, but also some trace elements in coal are also transported and released into the atmosphere [2]. These trace elements include mercury, arsenic lead and other heavy metals. Among them, arsenic has attracted much attention due to its extremely strong toxicity and carcinogenicity [3-4].

It is generally believed that arsenic volatilizes from the inside of carbon particles into flue gas in the process of coal combustion, and the temperature of flue gas decreases continuously in the process of flowing from the furnace outlet to the tail flue. Arsenic in flue gas gradually changes from gas to solid phase, and forms and valence states migrate and change [5-7]. Arsenic with different forms has different harm to the environment. Therefore, studying the speciation change of arsenic during coal combustion is helpful to reveal the migration and transformation characteristics of arsenic and provide certain theoretical basis for arsenic emission control. Contreras, et al [8]. Through HSCChemistry and Simulating the Speciation Changes of Arsenic in Coal Combustion, it is found that when the temperature is higher than 1073K, arsenic mainly exists as ASO<sub>2</sub>(g) and ASO (g) Liu Yinghui et al. [9] using Chemical Heat Balance Software and FACT analyzed the transformation of arsenic form in coal combustion in reducing and oxidizing atmosphere. The results showed that in reducing atmosphere, 700–800K appeared gaseous elemental arsenic. After the temperature further increased, the main product of arsenic was ASO (g). Under oxidizing atmosphere, when higher than 800K, the main products are ASO (g). Urban and et al. [10] calculated and compared the energy of the reaction of As with oxygen by using Gaussian Software under Different Methods / Basic Group Conditions Monahan-Pendergast et al. [11] studied the Reaction Mechanism of As and Some Free Radicals (OH, HO<sub>2</sub> Etc.). Urban and et al. [12] using Density Functional Theory and Ab initio Calculation Method, studied the Reaction Kinetics between As and HCl in Coal Fired Flue Gas.

During coal combustion, flue gas contains a large amount of nitrogen oxides, such as N<sub>2</sub>O, NO<sub>2</sub> and NO. Many scholars have studied the release characteristics of nitrogen oxides [13-15], and found that nitrogen oxides can undergo

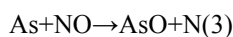
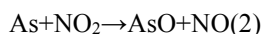
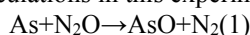
redox reactions with other gases or coke. Therefore, nitrogen oxides in flue gas may react with arsenic in gas phase, but there are few reports on this aspect. Limited to the current measurement level, it is difficult to directly measure the release mechanism of arsenic in the combustion process, and the content of arsenic released in the combustion process is less, the chemical reaction time is very short, and it is difficult to accurately determine the reaction mechanism by experiments. Quantum chemical calculation is an effective means to calculate molecular geometric structure and reaction mechanism [16-17] simulates chemical reaction process with computer under the theoretical framework of quantum mechanics, and provides theoretical basis for further study of arsenic release and migration during coal combustion by calculating kinetic and thermodynamic parameters.

In this study, three nitrogen oxides ( $N_2O$ ,  $NO_2$  and  $NO$ ) were selected in the combustion process, and their reactivity with arsenic was studied by density functional theory.

## 1. Computational Theory

### 1.1 Theoretical Methods and Basic Groups

Quantum chemistry method is a theoretical method to accurately calculate molecular configuration and energy, and density functional theory has been widely used in quantum chemistry calculation. In this study, the density functional theory method of B3LYP and 6-311G\* are used to study the micro-mechanism of arsenic and oxygen-containing gas reaction during coal combustion. The optimized Reactant(abbreviated as R), TransitionState(Abbreviated as TS), Intermediate(abbreviated as M) and Product (abbreviated as P) configurations, and the authenticity of each structure is verified through frequency calculation results and zero correction energy (ZPE) is obtained. There is only one imaginary frequency in transition states, and the vibration direction of the imaginary frequency points to the reaction direction and passes through the intrinsic reaction coordinates IRC(Intrinsic Reaction Coordination) to calculate and verify the correlation between reactants, intermediates, transition states and products. The energy calculation adopts B2PLYP method in double hybrid functional and def2-QZVPP basis set. Zero-point energy correction is considered in the energy calculation process. All calculations in this experiment are done by Gaussian09 package [18]. The reaction studied is as follows:



### 1.2 Dynamic Parameter Calculation Method

The reaction rate constant of the classical transition state is calculated as follows [19]:

$$k = k_T \times \frac{k_B T}{h} \times \frac{Q_{TS}}{Q_A Q_B} \times \exp\left(\frac{-E_a}{RT}\right) \quad (4)$$

Where  $k_T$  is the quantum tunnel correction coefficient;  $k_B$  is Boltzmann constant, J/K,  $h$  is planck constant, J·s,  $Q_{TS}$ ,  $Q_A$ ,  $Q_B$  are partition functions of transition state TS, reactant A and reactant B respectively;  $E_a$  is the reaction activation energy, kJ/mol;  $R$  is the gas molar constant, j/(mol k);  $T$  is thermodynamic temperature, k. Among them, the calculation formula of quantum tunnel correction coefficient is as follows:

$$k_T = 1 + \left(\frac{1}{24}\right) \times \left(\frac{h\nu_m c}{k_B T}\right)^2 \quad (5)$$

Where  $\nu_m$  is the vibration frequency of the reaction path,  $cm^{-1}$ ,  $C$  is the speed of light, m/s.

## 2. Results and Discussions

### 2.1 Reaction Process

Using B3LYP method, potential energy surface scanning is carried out at the level of 6-311G\* basic group, and then saddle point corresponding structures on the potential energy surface are obtained as initial guesses to search for transition

states. Then, optimize the geometric configuration of all stagnation points on the reaction channel to obtain the microscopic process of the reaction, as shown in the figure 1- figure 3.

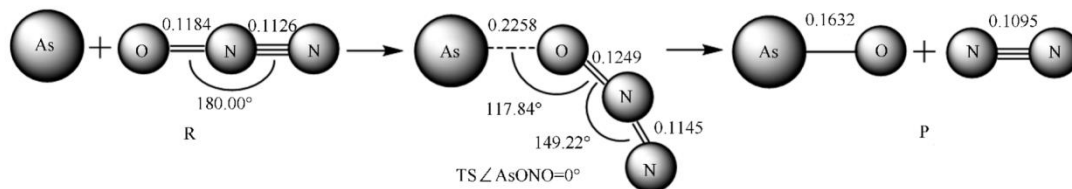


Figure1 Reaction process analysis of  $\text{As} + \text{N}_2\text{O} \rightarrow \text{AsO} + \text{N}_2$

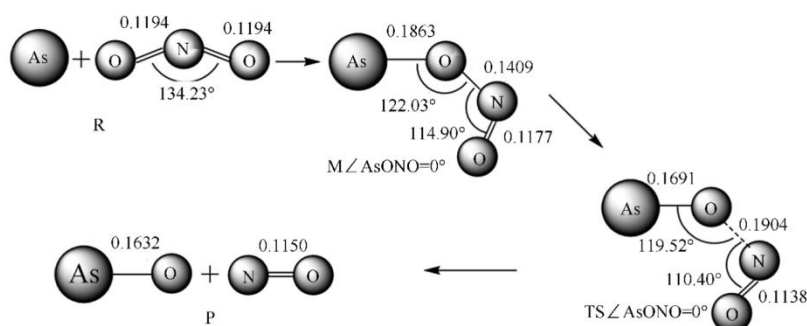


Figure2 Reaction process analysis of  $\text{As} + \text{NO}_2 \rightarrow \text{AsO} + \text{NO}$

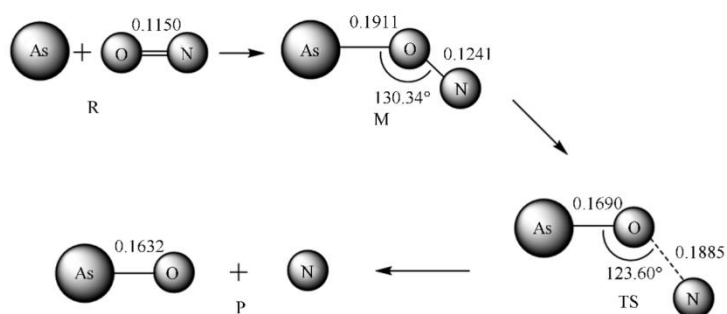


Figure3 Reaction process analysis of  $\text{As} + \text{NO} \rightarrow \text{AsO} + \text{N}$

As can be seen from fig. 1, the process of the reaction formula (1) is:  $\text{As} + \text{N}_2\text{O} \rightarrow \text{TS}(\text{AsONN}) \rightarrow \text{AsO} + \text{N}_2$ , i.e. as and o atoms combine to form a transition state

TS, and then form a product  $\text{AsO} + \text{N}_2$ . no intermediate is generated, only a transition state exists, which is a one-step reaction. In the course of the reaction, as-o the length of the bond gradually decreases ( $\infty \rightarrow 0.2258 \text{ nm} \rightarrow 0.1632 \text{ nm}$ ,  $\infty$  means the distance exceeds the bonding range), O-N and the length of the bond gradually increases ( $0.1184 \text{ nm} \rightarrow 0.1249 \text{ nm} \rightarrow \infty$ ), which shows that the formation of As-O bond and the fracture of O-N bond are simultaneous. Vibration analysis results show that the transition state has only one imaginary frequency ( $-617.22 \text{ cm}^{-1}$ ), in the virtual frequency vibration mode, the O atom has significant vibration along the reaction coordinate toward the As atom, which

indicates that the transition state is accurate.

As can be seen from fig. 2, the process of the reaction formula (2) is:  $\text{As} + \text{NO}_2 \rightarrow \text{M}(\text{AsONO}) \rightarrow \text{TS}(\text{AsONO}) \rightarrow \text{AsO} + \text{NO}$ , i.e., the O atoms of AS and NO<sub>2</sub> combine to generate stable intermediate M, and then M generates products ASO and NO via the transition state TS. In the course of the reaction, The length of the As-O bond is gradually reduced ( $\infty \rightarrow 0.1863\text{nm} \rightarrow 0.1691\text{nm} \rightarrow 0.1632\text{nm}$ ), and the length of the O-N bond is gradually increased ( $0.1194\text{nm} \rightarrow 0.1409\text{nm} \rightarrow 0.1904\text{nm} \rightarrow \infty$ ), which reflects the formation of As-O bond, while the adjacent O-N bond breaks. The change of molecular structure reflects the microscopic process of the reaction. Vibration analysis results show that the vibration frequency of the intermediate is all positive and is a stable point on the potential energy surface. Vibration analysis of transition state shows that there is only one imaginary frequency ( $-175.84\text{cm}^{-1}$ ), and the vibration direction of the imaginary frequency points to the reaction direction.

As can be seen from fig. 3, the process of reaction formula (3) is:  $\text{As} + \text{NO} \rightarrow \text{M}(\text{AsON}) \rightarrow \text{TS}(\text{AsON}) \rightarrow \text{AsO} + \text{N}$ . In the reaction, the length of as-o bond gradually decreases ( $\infty \rightarrow 0.1911\text{nm} \rightarrow 0.1690\text{nm} \rightarrow 0.1632\text{nm}$ ), indicating the gradual formation of As-O bonds. The length of O-N bond gradually increases ( $0.1150\text{nm} \rightarrow 0.1241\text{nm} \rightarrow 0.1885\text{nm} \rightarrow \infty$ ),

indicating that O-N and bond gradually breaks. Vibration analysis results show that the vibration frequency of the intermediate is all positive and is the stable point on the potential energy surface. Vibration analysis of transition state shows that there is only one imaginary frequency ( $-643.62\text{cm}^{-1}$ ), indicating that the transition state is credible and the reaction mechanism studied is reasonable.

The molecular structures of the reactants and products obtained through optimization are shown in Table 1. From the table 1, it can be seen that the parameters of stable structures of each molecule calculated by B3LYP method in density functional theory are in good agreement with experimental values.

Table 1 Calculated and experimental bond lengths and bond angles

Species	Bond length ( $r/\text{nm}$ )	Calculated value	Experimental value
	Bond angle ( $\theta/(\text{ }^\circ)$ )		
$\text{N}_2\text{O}$	$r(\text{N-O})$	0.1184	0.1185 <sup>[20]</sup>
	$r(\text{N-N})$	0.1126	0.1127 <sup>[20]</sup>
	$\theta(\text{N-N-O})$	180.00	180.00 <sup>[20]</sup>
$\text{N}_2$	$r(\text{N-N})$	0.1095	0.1098 <sup>[20]</sup>
$\text{NO}_2$	$r(\text{N-O})$	0.1194	0.1199 <sup>[21]</sup>
	$\theta(\text{O-N-O})$	134.23	133.70 <sup>[21]</sup>
$\text{NO}$	$r(\text{N-O})$	0.1150	0.1151 <sup>[22]</sup>
$\text{AsO}$	$r(\text{As-O})$	0.1632	0.1624 <sup>[23,24]</sup>

## 2.2 Energy Changes in Reaction Process

The energy, zero energy, total energy  $E_{\text{tot}}$  of the reactants, intermediates, transition states and products (the energy calculated by B2PLYP/def2-QZVPP plus zero energy) and the relative energy  $E_{\text{rel}}$  based on the reactants are shown in Table 2.

According to the transition state theory, the activation energy is the energy difference between the transition state and the stable reactant (or intermediate). From Table 2, it can be seen that the activation energies of the three reactions are 78.45, 2.58, 155.85kJ/mol, the activation energy of the reaction (2) is the lowest, indicating that the reaction is easy to carry out. This is because NO<sub>2</sub> has strong oxidation[25], which is easy to oxidize arsenic into AsO during the reaction process. However, NO is a relatively stable gas, which needs to overcome a large amount of energy to break N-O and bond. In the course of the reaction, the bond length in the system changes continuously, that is, the energy of its system also changes continuously. For example, reaction (1), when As atom approaches O atom forms transition state, As-O bond has strong effect and system energy increases. The transition state and the AS-O bond length of the product are 0.2258 and 0.1632nm, and the energy of the corresponding system is  $-2420.15112(\text{a.u.})$  and  $-2420.32382(\text{a.u.})$ . It can be seen that AS-O and bond length change determine the energy of the system.

Table 2 Stationary point energy of each reaction

	Reaction	B2PLYP/( a.u.)	ZPE/( a.u.)	$E_{tot}$ /( a.u.)	$E_{rel}$ /( $\text{kJ}\cdot\text{mol}^{-1}$ )
( 1 )	As+N <sub>2</sub> O	-2420.19225	0.01125	-2420.18100	0
	TS	-2420.15981	0.00869	-2420.15112	78.45
	AsO+N <sub>2</sub>	-2420.33202	0.00820	-2420.32382	-374.97
( 2 )	As+NO <sub>2</sub>	-2440.60933	0.00882	-2440.60051	0
	M	-2440.68649	0.00904	-2440.67745	-202.01
	TS	-2440.68426	0.00779	-2440.67647	-199.43
	AsO+NO	-2440.69733	0.00727	-2440.69006	-235.11
( 3 )	As+NO	-2365.42302	0.00453	-2365.41849	0
	M	-2365.41799	0.00425	-2365.41374	12.47
	TS	-2365.35649	0.00211	-2365.35438	168.32
	AsO+N	-2365.38994	0.00247	-2365.38747	81.44

## 2.3 Dynamic Analysis

Calculate the reaction rate and pre-exponential factor of each reaction under 298, 600, 900, 1200, 1500, 1800K according to the classical transition state theory. The calculated results are shown in Table 3- Table 5.

Table 3 Kinetic parameters of the reaction  
As+N<sub>2</sub>O→AsO+N<sub>2</sub> at different temperatures

$T/\text{K}$	$A/(\text{cm}^3\cdot\text{mol}^{-1}\cdot\text{s}^{-1})$	$k/(\text{cm}^3\cdot\text{mol}^{-1}\cdot\text{s}^{-1})$
298	$6.48\times 10^{10}$	$1.15\times 10^{-3}$
600	$8.76\times 10^{10}$	$1.30\times 10^4$
900	$1.05\times 10^{11}$	$2.95\times 10^6$
1200	$1.19\times 10^{11}$	$4.57\times 10^7$
1500	$1.29\times 10^{11}$	$2.39\times 10^8$
1800	$1.37\times 10^{11}$	$7.26\times 10^8$

Table 4 Kinetic parameters of the reaction  
As+NO<sub>2</sub>→AsO+NO at different temperatures

$T/\text{K}$	$A/(\text{cm}^3\cdot\text{mol}^{-1}\cdot\text{s}^{-1})$	$k/(\text{cm}^3\cdot\text{mol}^{-1}\cdot\text{s}^{-1})$
298	$8.52\times 10^{12}$	$3.02\times 10^{12}$
600	$1.47\times 10^{13}$	$8.80\times 10^{12}$
900	$1.82\times 10^{13}$	$1.29\times 10^{13}$
1200	$2.03\times 10^{13}$	$1.57\times 10^{13}$
1500	$2.17\times 10^{13}$	$1.77\times 10^{13}$
1800	$2.27\times 10^{13}$	$1.92\times 10^{13}$

From Table 3- Table 5, it can be seen that with the increase of temperature, the pre-exponential factor reaction rate of each reaction gradually increases, but the increase amplitude of different reactions is different. In the considered temperature range, the rate of reaction ( 2 ) is always greater than 10<sup>12</sup>, which indicates that the reaction is extremely fast. Reaction (1) from  $1.15\times 10^{-3}$  increased to  $7.26\times 10^8$ . Reaction (3) from  $4.95\times 10^{-15}$  increased to  $9.33\times 10^8$ .

Table 5 Kinetic parameters of the reaction  
As+ NO→AsO+ N at different temperatures

T/K	A/(cm <sup>3</sup> •mol <sup>-1</sup> •s <sup>-1</sup> )	k/(cm <sup>3</sup> •mol <sup>-1</sup> •s <sup>-1</sup> )
298	1.02×10 <sup>13</sup>	4.95×10 <sup>-15</sup>
600	1.80×10 <sup>13</sup>	4.88×10 <sup>-1</sup>
900	2.31×10 <sup>13</sup>	2.09×10 <sup>4</sup>
1200	2.66×10 <sup>13</sup>	4.38×10 <sup>6</sup>
1500	2.92×10 <sup>13</sup>	1.09×10 <sup>8</sup>
1800	3.11×10 <sup>13</sup>	9.33×10 <sup>8</sup>

Logarithms are taken from both sides of  $k = a \exp(-ea/rt)$ , i.e.  $\ln k = \ln a - (ea/rt)$ , with  $1000/T$  as the abscissa and  $\ln k$  as the ordinate to show the data of each reaction in the same coordinate, as shown in fig. 4. As can be seen from fig. 4(a),  $\ln k$  and  $1000/T$  show a good linear relationship. Fig. 4(b) shows the variation trend of  $\ln k$  of each elementary reaction with temperature. From the graph 4(B), it can be seen that each reaction rate curve increases with the increase of temperature, which is consistent with the reduction of nitrogen oxides studied by other scholars [26]. The reaction rate curve of reaction (2) is less affected by temperature, and the reaction is completed instantly within the considered temperature range. It can be seen from the kinetic parameters that the reaction rate is always at a higher level within the studied temperature range, i.e. the change of the reaction rate with temperature is small. In addition, because the high activity and strong oxidation of NO<sub>2</sub> [25], it can quickly form a stable intermediate with elemental arsenic, and the intermediate only needs to overcome a small energy barrier to finally obtain a product, indicating that the reaction is extremely easy to occur. For the reactions (1) and (3), at 298–900K, the reaction rate increases rapidly with the change of temperature, and when the temperature further increases, its increasing trend slows down.

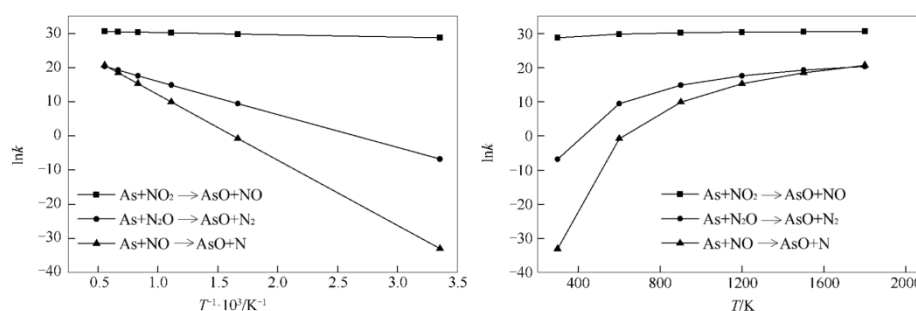


Figure4 Values of  $\ln k$  at different temperatures for each reaction

The kinetic parameters of 3 kind of reaction rate constant curve are obtained by linear fitting. The specific results are shown in table 6.

Table 6 Kinetic parameters for each reaction

Reaction	A/(cm <sup>3</sup> •mol <sup>-1</sup> •s <sup>-1</sup> )	E <sub>a</sub> / (kJ•mol <sup>-1</sup> )
As+N <sub>2</sub> O→AsO+N <sub>2</sub>	1.48×10 <sup>11</sup>	78.45
As+NO <sub>2</sub> →AsO+NO	2.72×10 <sup>13</sup>	2.58
As+NO→AsO+N	3.69×10 <sup>13</sup>	155.85

### 3. Conclusion

The activation energy of  $\text{As} + \text{NO}_2 \rightarrow \text{AsO} + \text{NO}$  is 2.58 kJ/mol, indicating extremely fast response. The activation energy of  $\text{As} + \text{N}_2\text{O} \rightarrow \text{AsO} + \text{N}_2$  is 78.45 kJ/mol, the activation energy of  $\text{As} + \text{NO}_2 \rightarrow \text{AsO} + \text{NO}$  is 155.85 kJ/mol and higher activation energy indicate that the reaction is relatively slow.

In the reaction process, the bond lengths of As-O and As-O in the system mainly determine the energy of different structures. The change of bond lengths between atoms in the system reflects the microscopic process of the reaction.

The reaction rate curves of As, and  $\text{NO}_2$  are less affected by temperature, and the reaction is completed instantaneously within the considered temperature range. However, in the reaction of 298–900K, arsenic and  $\text{N}_2\text{O}$ , and  $\text{NO}$ , the reaction rate increases rapidly with the change of temperature. When the temperature increases further, the increasing trend slows down.

Quantum chemical calculation is an effective method to study reaction mechanism. The reaction process between arsenic and nitrogen oxides reveals the morphological changes of arsenic during coal combustion, which provides a theoretical basis for more economical and effective control of arsenic emissions.

## References

1. Li Wenxiu, Wang Baofeng, Ren Jie, Zhang Qian, Fengling Yang, Cheng Fangqin. Effects of intrinsic minerals on  $\text{SO}_2$  and  $\text{NO}_x$  emission characteristics during lean coal combustion in  $\text{O}_2/\text{CO}_2$  atmosphere [J]. *Journal of Fuel Chemistry*, 2017,45(10):1200–1208.
2. WANGC, LIUH,ZHANGY, ZOUC, ANTHONY EJ. Review of arsenic behavior during coal combustion: Volatilization, transformation, emission and removal technologies[J]. *Prog Energy Combust*, 2018, 68:1–28.
3. LIUH, PANW, WANGC, ZHANGY. Volatilization of arsenic during coal combustion based on isothermal-thermogravimetric analysis at 600–1500 °C [J]. *Energy Fuels*, 2016, 30(8):6790–6798.
4. LIUH,WANGC,ZOUC,ZHANGY,WANGJ. Simultaneous volatilization characteristics of arsenic and sulfur during isothermal coal combustion [J]. *Fuel*, 2017, 203:152–161.
5. TANGQ, LIUGJ, ZHOUC, SUNRY. Distribution of trace elements in feed coal and combustion residues from two coal-fired power plants at Huainan, Anhui, China [J]. *Fuel*, 2013, 107:315–322.
6. ZHAOY, ZHANGJ, HUANGW, WANGZ, LIY, SONGD, ZHAOF, ZHENG C. Arsenic emission during combustion of high arsenic coals from Southwestern Guizhou, China [J]. *Energy Convers Manage*, 2008, 49(4):615–624.
7. ZIELINSKIRA, FOSTERAL, MEEKERGP, BROWNFIELDIK. Mode of occurrence of arsenic in feed coal and its derivative flyash, Black Warrior Basin, Alabama [J]. *Fuel*, 2007, 86(4):560–572.
8. CONTRERASML, AROSTEGUIJM, ARMESTOL. Arsenic interactions during co-combustion processes based on thermodynamic equilibrium calculations [J]. *Fuel*, 2009, 88:539–546.
9. Liu Yinghui, Zheng Chuguang, You Xiaoqing, Guo Xin. Interaction of Volatile and Toxic Trace Elements in Coal Burning Process [J]. *Combustion Science and Technology*, 2001, 7(4):243–247.
10. URBANDR, WILCOXJ. A theoretical study of properties and reactions involving arsenic and selenium compounds present in coal combustion flue gases [J]. *J Phys Chem A*, 2006, 110(17):5847–5852.
11. MONAHAN-PENDERGASTM, PRZYBYLEKM, LINDBLADM, WILCOXJ. Theoretical prediction of arsenic and selenium species under atmospheric conditions [J]. *Atmos Environ*, 2008, 42(10):2349–2357.
12. URBANDR, WILCOXJ. Theoretical study of the kinetics of the reactions  $\text{Se} + \text{O}_2 \rightarrow \text{Se} + \text{O}$  and  $\text{As} + \text{HCl} \rightarrow \text{AsCl} + \text{H}$  [J]. *J Phys Chem A*, 2006, 110(28):8797–8801.
13. Thunder, Huang Xingzhi, Wang Chunbo. Characteristics of  $\text{NO}$  Formation during Medium-High Temperature Combustion of Typical Coal Type  $\text{O}_2/\text{CO}_2/\text{H}_2\text{O}$  Atmosphere [J]. *Journal of Dynamic Engineering*, 2017, 37(6):432–439.
14. Wang Chunbo, Yue Shuang, Xu Xubin, Li Yipeng.  $\text{O}_2/\text{CO}_2$  Constant Temperature Combustion of Coal Char in Atmosphere  $\text{NO}_x$  Release Characteristics [J]. *Journal of Coal*, 2018, 43(1): 257–264.
15. Xiao Haiping, Zhou Junhu, Liu Jianzhong, Baomin Sun, Ye Liping. Effect of Sulfur Compounds on  $\text{NO}$  Reduction Process [J]. *Journal of Fuel Chemistry*, 2008, 36(3):381–384.
16. Liu Jing, Zheng Chuguang, Qiu Jianrong. Study on Quantum Chemical Calculation Method of Mercury Reaction in Combustion Smoke [J]. *Journal of Engineering Thermophysics*, 2007, 28(3):519–522.
17. AWUAHAJB, DZADENY, TIAR, ADEIE, KWAKYE-AWUAHADB, CATLOWCRA, DELEEUWNH. A density functional theory study of arsenic mobilization by the Al(III)-modified zeolite clinoptilolite [J]. *Phys Chem Chem Phys*, 2016, 18(16):11297–11305.
18. FRISCHMJ, TRUCKSGW, SCHLEGELHB. Gaussian09, Revision D. 01 [J]. Gaussian, Inc., Wallingford, CT, 2009.
19. ZHANGH, LIUJ, SHENJ, JIANGX. Thermodynamic and kinetic evaluation of the reaction between  $\text{NO}$  (nitric oxide) and char(N) (char bound nitrogen) in coal combustion [J]. *Energy*, 2015, 82(C): 312–321.

20. SCHRDERB, SEBALDP, STEINC, WESERO, BOTSCHWINAP. Challenging high-level abinitio rovibrational spectroscopy: The nitrous oxide molecule [J]. *ZPhysChem*, 2015, 229(10/12):1663–1690.
21. BORISENKOKB, KOLONITSM, ROZSONDAIB, HARGITTAI. Electron diffraction study of the nitrous oxide molecular structure at 294, 480, and 691 K [J]. *JMolStruct*, 1997, 413–414:121–131.
22. MARSDENCJ, SMITHBJ. Abinitio force constants: A cautionary tale concerning nitrogen oxides [J]. *JMolStruct: Theochem*, 1989, 187:337–357.
23. EVENSONKM, WELLSJS, RADFORDHE. Infrared resonance of OH with the H<sub>2</sub>O laser: A galactic maser pump? [J]. *Phys Rev Lett*, 1970, 25(4): 199–202.
24. MIZUSHIMAM. Molecular parameters of OH free radical [J]. *Phys Rev A*, 1972, 5(1):14-157.
25. Wang Penggan, Wang Changan, Du Yongbo, Zhang Longfei, Chedafu. Experimental Study on Reduction Characteristics of O<sub>2</sub>/CO<sub>2</sub> Under Combustion Conditions NO<sub>2</sub> [J]. *Journal of Xi'an Jiaotong University*, 2017, 51(5):16–22.
26. JIAOA, ZHANGH, LIUJ, SHENJ, JIANGX. The role of CO played in the nitric oxide heterogeneous reduction: A quantum chemistry study [J]. *Energy*, 2017, 141:1538–1546.